Implementation of Charge-Pump Active-Matrix OLED Panel with 64 x 64 Pixels Using ITO/SiO$_2$/ITO Capacitors and a-Si:H Schottky Diodes

Se-Hwan Na, Jong-Wook Seo
Dept. of Electronic, Information and Communications Engineering, Hongik Univ, 72-1, Sangsu-dong, Mapo-gu, Seoul 121-791, Korea

Mi-Young Kwak, Jae-Hoon Shim
Gracel Display Inc.,
5F Samyangtechnotown, 284-25 Seongsu 2-ga, Seongdong-gu, Seoul 133-833, Korea
Tel : +82-2-320-1663 ; E-mail : jwseo@wow.hongik.ac.kr

Abstract

Organic light-emitting diode (OLED) display panel with 64 × 64 pixels utilizing the charge-pump (CP) pixel addressing method was fabricated using conventional thin-film processes. Each pixel consists of a-Si:H Schottky diode and ITO/SiO$_2$/ITO capacitor. It is shown that CP-OLED is technically feasible for information display and a driving voltage below 4V$_{pp}$ is enough for nominal operation.

1. Introduction

An OLED is one of the most promising technologies in flat-panel display area due to its unique characteristics, including light-weight, wide viewing angle, self-emission, thinness and rapid response [1]. Amongst these benefits, the potential of low manufacturing cost can be regarded as the most important one, and it is rooted in its simple structure compared to other competing technologies. However a high information-density display requires not only the formation of OLEDs, but also the spatial separation and addressing of pixels [2]. Although a great effort has been put in to bring the TFT-based AM-OLED display into the market, the OLED still has problems to be resolved such as threshold voltage shifts of TFTs [3] the loss of aperture ratio due to the circuit complexity [4], and the insufficient lifetime [5].

A new easy-to-make charge-pump pixel circuit consisting of a storage capacitor and a rectifying diode has been proposed [6]-[8]. The new method provides a way to eliminate the need for the complex TFT-based pixel circuits. The basic operation of the circuit is to pump a fixed amount of charge into an OLED, and consequently drive an electrical current through the OLED during most of the frame period as in the TFT-based AM-OLED. Figure 1 shows the schematic representation of the two-dimensional OLED cell array with charge-pump pixel circuits. In this paper, we investigate and discuss the fabrication of an OLED panel with 64 × 64 pixels adopting the new addressing method and its operation characteristics were analyzed.
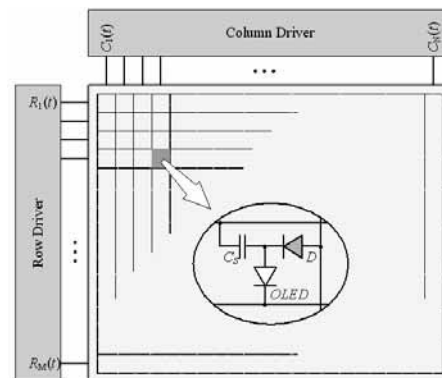

Fig. 1. Schematic representation of $M \times N$ OLED cell array with charge-pump pixel drivers.

2. Fabrication & Experiments

A CP-OLED panel with 64 × 64 pixels was fabricated by using conventional thin-film processes. The storage capacitors each of which covers the whole area of a pixel with an area of 490 × 490 μm^2 were formed by PECVD deposit of a 700 Å thick SiO$_2$ layer sandwiched between the row-bus lines (ITO) and the floating common electrodes (ITO). The rectifying Schottky diodes with an area of 100 × 50 μm^2 were formed by a 3000 Å thick hydrogenated amorphous silicon layer, which was deposited by PECVD. Figure 2(a) shows the photograph and cross-sectional view of a pixel and it can be shown from the figure that light emits only from the area depicted as

OLED window, which has an area of $190 \times 310 \ \mu m^2$. The OLED used in this study has a thickness of 1230 Å and the thickness of a common cathode electrode consisting of Al is 1000 Å. Figure 2(b) shows the fabricated CP-OLED panel finished with encapsulation and flexible printed circuit (FPC) cable bonding.
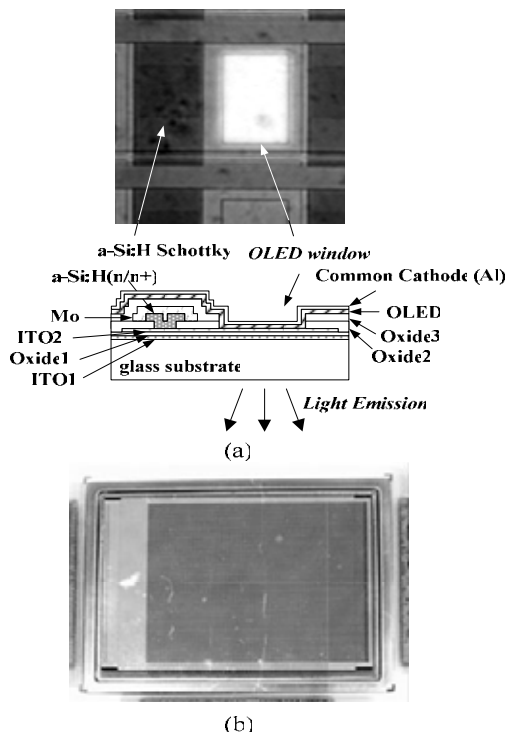

(a)

(b)

Fig. 2. (a) The photograph and cross-sectional view of the pixel. The pixel is turned on by injecting current. (b) Photograph of a panel completed with encapsulation and FPC (Flexible Printed Circuit) cable bonding.

Since the controller is with a limited number of gates, the panel was subdivided into common-circuited 2×2 array of 32×32 pixel arrays. Control signals with a scan period of 65 μs and a charging time of 2 μs were required to drive the 32×32 pixel array to perform an 8-bit gray scale with a frame rate of 60 fps. The gray scale control can be achieved using a method similar to the pulse width modulation (PWM) where the total number of charge-pumping during a frame period is controlled [6]-[8].

3. Results and Discussions

Figure 3 shows the CP-OLED panel driven to display a test image. As can be seen from the figure, the charge-pump pixel addressing method operates properly to display images. The line defects on top of the image are due to the incomplete contact between the panel and the FPC connectors, and the areal defects on the top left corner are due to the accidental over-voltage burn out occurred while setting up the operating conditions. The point defects were found to be mostly due to the electrostatic discharge (ESD). The bad section with darker pixels around the low right corner of the panel is believed to be due to the process fault that is related specifically to the a-Si:H deposition. Despite the foregoing unskillful conditions of the panel, it can be seen that the CP-OLED panel can be implemented by using the conventional thin-film processes.
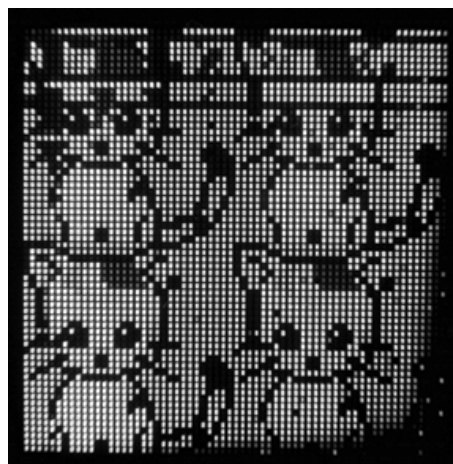

Fig. 3. Photograph of an OLED panel with 64×64 pixels displaying a test image. The panel was subdivided into common-circuited 2×2 array of 32×32 pixel arrays.

Considering that the pixel size scales down with the panel resolution, this method can be accepted as a suitable method for implementing high-information density OLED panels. The capacitive load for the drive circuit in a panel would not increase with the pixel density as smaller pixels are used. Meanwhile, it was found that the relative brightness of the pixels is expressed differently from the original gray-scale data, and the deviation was found to be due to the crosstalk between pixels caused by the overlap capacitance between the column bus and the common electrode [8].

The overlap capacitance between the column-bus and the floating common electrode, the storage capacitance, and the row- and column-bus line resistance were measured using an HP 4192A impedance analyzer. Since the row-bus line and the storage capacitance are connected in series as shown in Fig. 4(a), the row-bus line resistance R_{row} and the storage capacitance C_s can be obtained from the real and imaginary part of the measured impedance,

respectively. Figure 5(a) shows the measured storage capacitances for some pixels across the panel. From the figure, it can be seen that the storage capacitance values distribute with a moderate uniformity at around 180 pF. In addition, the dielectric layer of the capacitors withstands the operating voltage of up to 10 V.
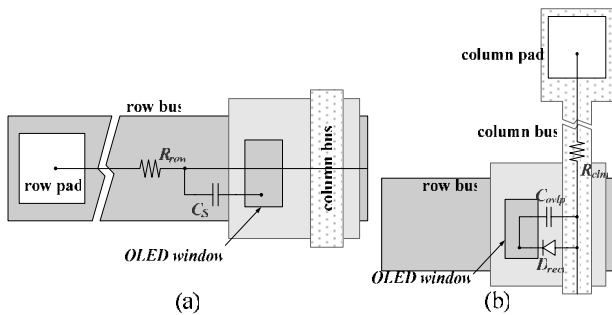

Fig. 4. Schematic representation of electrical connection between an FPC contact pad and an OLED window of a pixel for (a) row and (b) column bus line.
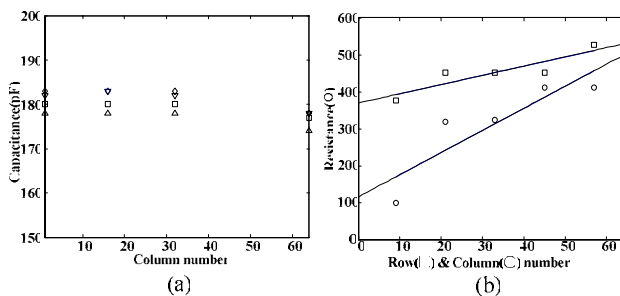

Fig. 5. (a) Measured storage capacitances of a CP-OLED backplane with 64 × 64 pixels along the 1st(□), 16th(◇), 32nd(△), and 64th(▽) row. Measurement was made at a frequency of 100 kHz. (b) Measured line resistances of row (□) and column (○) bus.

Since the column-bus line and the overlap capacitance are connected in series as shown in Fig. 4(b), the column-bus line resistance R_{clm} and the overlap capacitance C_{ovlp} can also be obtained in the similar way. Considering that the amplitude of the test signal for the impedance measurement is small enough to keep the diode from turning on and the diode junction capacitance is much smaller than the overlap capacitance, the effect of the a-Si:H diode can be ignored. The overlap capacitances were also found to have uniform values of about 130 pF. Figure 5(b) shows the measured line resistances for the row- and column-bus. The abscissa is the column- and row-line number for the row- (□) and column-bus (○) resistance, respectively, and the slope is the bus line resistance per unit pixel. From the Fig. 5(b), it can be

seen the bus resistance for row and column bus is 2.3 Ω /pixel and 5.9 Ω /pixel, respectively.

The *I-V* characteristics of the a-Si:H Schottky diodes were measured using the configuration shown in Fig. 4(b), and the diode turn-on voltages were found to have a large inhomogeneity across the panel as can be seen from Fig. 6(a). The saturation currents of the diodes were extracted from the *I-V* data and were found to be uniform with a value of *IS*=50 pA as shown Fig. 6(b), whereas the ideality factor *N* and the series resistance R_S were found to vary drastically from 7.5 to 18.4 and from 60 kΩ to 110 kΩ as can be seen in Fig. 6(c) and (d), respectively, across the panel. It means that the uniformity of the diode characteristics depends mainly on the electrical properties of the lightly-doped amorphous silicon and the junction formed with the metal (Mo) on it. [7]
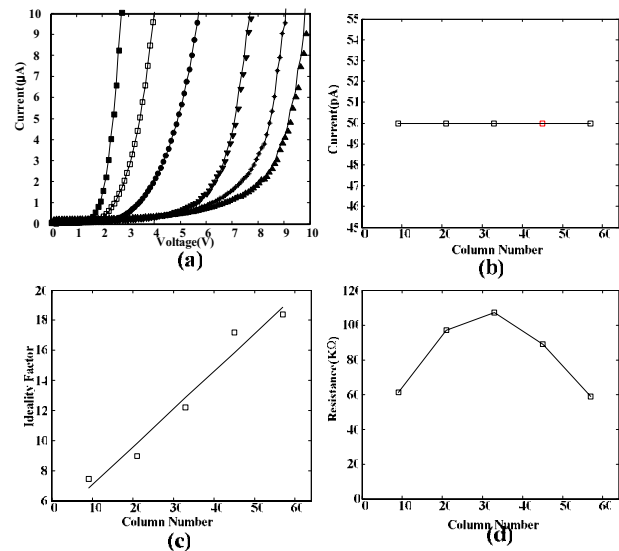

Fig. 6. (a) Measured *I-V* characteristics of a-Si:H Schottky diodes at the 9th(■), 21st(●), 33rd(▼), 45th(*), and 57th(▲) row along the 9th column line. Also shown is that of diodes at the 57th column of the 9th row. (b) Saturation currents and (c) Ideality factors measured from the *I-V* characteristics of a-Si:H Schottky diodes at the 9th, 21st, 33rd, 45th and 57th row along the 9th column line. (d) Series resistance of a-Si:H Schottky diodes at the 9th, 21st, 33rd, 45th, 57th row along the 9th column line from *I-V* characteristics.

The performance of the panel was characterized by analyzing the display pattern of an image with a uniform luminance as shown in Fig. 7. The display pattern from one of the subsections (32 × 32 pixels) was captured by a CCD camera (DTA Chroma-C3). The figure shows that the luminance variation is far more moderate than that of the a-Si:H Schottky diode

turn-on voltage [7]. The charge pump action by the storage capacitance lessens the dependence of the cell luminance on the device characteristics. It can also be seen that the display performance becomes less sensitive to the device characteristics when driven by control signals with larger amplitudes. It can also be seen that the panel luminance is highly dependent on the amplitudes of the control signals. That is, as the amplitude is increased from 3.0 V to 3.8 V, the panel luminance increases up to more than 6 times.

Meanwhile, the non-ideal behavior observed in gray scale representation such as non-linear dependence of the luminance on gray-level data and crosstalk between pixels are mainly related to the overlap capacitance that exists between the column-bus and the common electrode (ITO). Since the charge-pump circuit is activated by two switching of the rectifying diode, the overlap capacitance connected in shunt with the diode need to be minimized to maximize the voltage applied to the junction. It was found that the presence of the overlap capacitance results in loss of pixel luminance. The overlap capacitance also jeopardizes the electrical isolation between the column-bus and the common electrode resulting in crosstalk and loss of contrast ratio.
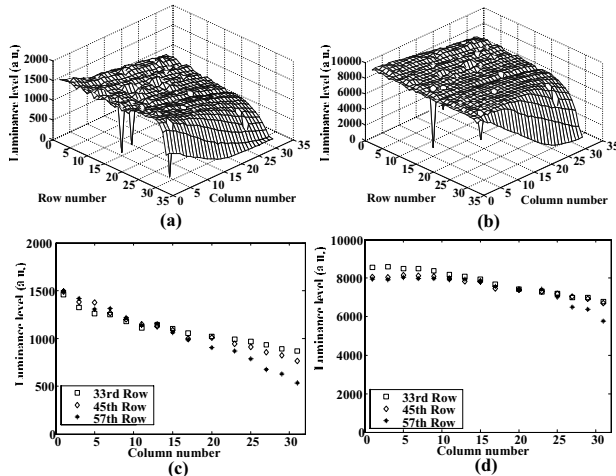

Fig. 7. Luminance variation for an "all white" image when driven by control signals with voltage amplitudes of (a) 3.0 V and (b) 3.8 V. The luminance variations along column lines at the 33rd(□), 45th(◇), and 57th(*) row are translated into line graphs for driving voltages of (c) 3.0 V and (b) 3.8V.

4.   Conclusions

Through this study, it was confirmed that the charge-pump pixel addressing can be applied to high information density OLED display panels. A CP-OLED panel with 64 × 64 pixels with an area of 490 × 490 μm^2 was fabricated and driven to display images. A CP-OLED pixel consists of a storage capacitor and an a-Si:H Schottky diode and the gray scale is controlled in a full digital way similar to the pulse width modulation. Although the performance of the panel is largely limited by the unripe processes, the devices fabricated using conventional thin-film processes have been verified to be suitable for implementation of CP-OLED panel. The panel was driven by control signals with voltage amplitude below 4 V. Considering that the panel brightness is sacrificed by the presence of the overlap capacitance, it is expected that the operating voltage can be reduced further for power efficient operation.

5.   Acknowledgements

6.   References

[1] P. E. Burrows, G. Gu, V. Bulović, Z. Shen, S. R. Forrest, and M. E. Thompson, IEEE Trans. Electron Devices, **44**, 1188 (1997).

[2] J. N. Bardsley, IEEE J. Sel. Topics Quantum Electron, **10**, 3 (2004).

[3] Y. C. Lin and H. P. D. Shieh, IEEE Trans. Electron Devices, **51**, 1037, (2005).

[4] H. S. Shin, J. H. Lee, S. H. Jung, C. Y. Kim, and M. K. Han, JID **6**, 12, (2005).

[5] M. K. Mathai and F. Papadimitrakopoulos, J. Appl. Phys. 95, 8240, (2004).

[6] J-W. Seo, H. Kim, B. Kim, and Y. Kim, Jpn. J. Appl. Phys. **41**, 7391, (2002).

[7] J-W. Seo, H. Kim, and C. Pyun, Jpn. J. Appl. Phys. **44**, 6571, (2005).

[8] S. H. Na, M. Y. Kwak, J. H. Shim and J. W. Seo, JID **7**, 35, (2006).